A Two-Phase Single-Reciprocating-Piston Heat Conversion Engine

Kirmse C.J.W., Taleb A.I., Oyewunmi O.A., Haslam A.J. and Markides C.N.*
*Author for correspondence
Clean Energy Processes (CEP) Laboratory, Department of Chemical Engineering,
Imperial College London,
London SW7 2AZ,
United Kingdom,
E-mail: c.markides@imperial.ac.uk

ABSTRACT

This paper considers an energy-conversion heat-engine concept termed 'Up-THERM'. This machine is capable of converting low- to medium-grade heat to useful positive-displacement work through the periodic evaporation and condensation of a working fluid in an enclosed space. These alternating phase-change processes drive sustained oscillations of thermodynamic properties (pressure, temperature, volume) as the working fluid undergoes an unsteady thermodynamic heat-engine cycle. The resulting oscillatory flow of the working fluid is converted into a unidirectional flow in a hydraulic load arrangement where power can be extracted from the machine.

The engine is described with lumped dynamic models constructed using electrical analogies founded on previously developed thermoacoustic and thermofluidic principles, which are extended here to include a description of the phase-change heat-transfer processes. For some sub-components of the engine, such as the gas spring, valves and the temperature profile in the heat exchangers, deviations from the linear theory are non-negligible. These are modelled using non-linear descriptions. In particular, the results of linear and non-linear descriptions of the gas spring are compared using three important performance indicators — efficiency, power output and frequency.

The non-linear description of the gas spring results in more-realistic predictions of the oscillation frequency compared to direct measurements on an experimental prototype of a similar engine. Owing to its mode of operation and lack of moving parts, the Up-THERM engine does offer a much simpler and more cost-efficient solution than alternative engines for heat recovery and solar applications. The results from this work suggest that this technology can be a competitive alternative in terms of cost per unit power in low-power, small-scale applications, especially in remote, off-grid settings, for example in developing countries where minimising upfront costs is crucial.

INTRODUCTION

In order to be competitive, low-power and small-scale power-generation applications need to have low capital and maintenance costs. Thermofluidic oscillators are suitable in this regard due to their few moving parts (and dynamic seals) and capability of converting low-grade heat sources, such as waste heat and low-temperature solar or geothermal heat, which are more affordable and easily accessible than higher-grade counterparts. Examples of thermofluidic oscillators currently under development include Fluidyne engines [1,2], thermoacoustic engines [3,4] and the 'Non-Inertive-Feedback Thermofluidic Engine' (NIFTE) [5-8].

The aim of the present study is to investigate a new heat-to-electricity energy-conversion concept termed 'Up-THERM', invented and owned by company Encontech B.V. (www.encontech.nl). The engine is being developed specifically for combined heat and power (CHP) applications under EU FP7 project Up-THERM (http://labor1.wix.com/up-therm) [9,10]. This heat-engine concept is a two-phase thermofluidic oscillator [5], which contains a single solid piston [9,10]. It utilizes the constant temperature difference between a heat source and heat sink to periodically evaporate and condense a working fluid in an unsteady thermodynamic cycle, leading to sustained oscillations of thermodynamic properties (pressure, temperature, volume). The resulting reciprocating vertical motion of the solid piston and oscillatory movement of the fluid are transformed through check valves and hydraulic accumulators into a unidirectional flow, which can be converted to useful work in a hydraulic motor.

One important part of the engine, which is found at its highest point, is the (vapour space) gas spring. For this component we develop linear (LG) *and* non-linear (NLG) descriptions of the gas spring, and proceed to compare both engine models according to three performance indicators: frequency, power output and exergy efficiency. For the NLG-model, we perform a parametric study and investigate the influence of the engine's physical dimensions on the three aforementioned performance indicators.

NOMENCLATURE

A	[m^2]	Cross-sectional area
C	[m^{4}s^2/kg]	Capacitance
d	[m]	Diameter
g	[m/s^2]	Gravitational acceleration
h	[m]	Height
k	[N/m]	Spring constant
L	[kg/m^4]	Inductance
l	[m]	Length
m	[kg]	Mass
P	[Pa]	Pressure
P_{hyd}	[W]	Power output
R	[kg/m^{4}s]	Resistance
U	[m^3/s]	Flow rate
V	[m^3]	Volume

Special characters

γ	[-]	Heat capacity ratio
δ	[m]	Gap between piston and slide bearing
ϵ	[m]	Gap between shaft and motor
η_{ex}	[-]	Exergy efficiency
μ	[m^2/s]	Dynamic viscosity
ρ	[kg/m^3]	Density

Subscripts

0	Equilibrium
a	Hydraulic accumulator
b	Slide bearing
c	Connection tube
cv	Check valve
d	Displacer cylinder
gen	Generator
hm	Hydraulic motor
l	Leakage flow
lub	Lubricant
p	Piston
pv	Piston valve
t	Tube
th	Thermal domain
v	Vapour space gas spring

Superscripts

*	Normalized value

ENGINE CONFIGURATION AND OPERATION

Figure 1 shows a schematic of the proposed Up-THERM engine concept. It comprises the displacer cylinder with the hot and cold heat exchangers, a solid piston which forms a 'piston-valve' arrangement with the cylinder wall, a slide bearing and a mechanical spring. The working fluid vapour at the top acts as a gas spring. The load arrangement contains two check (non-return) valves, hydraulic accumulators and a hydraulic motor.

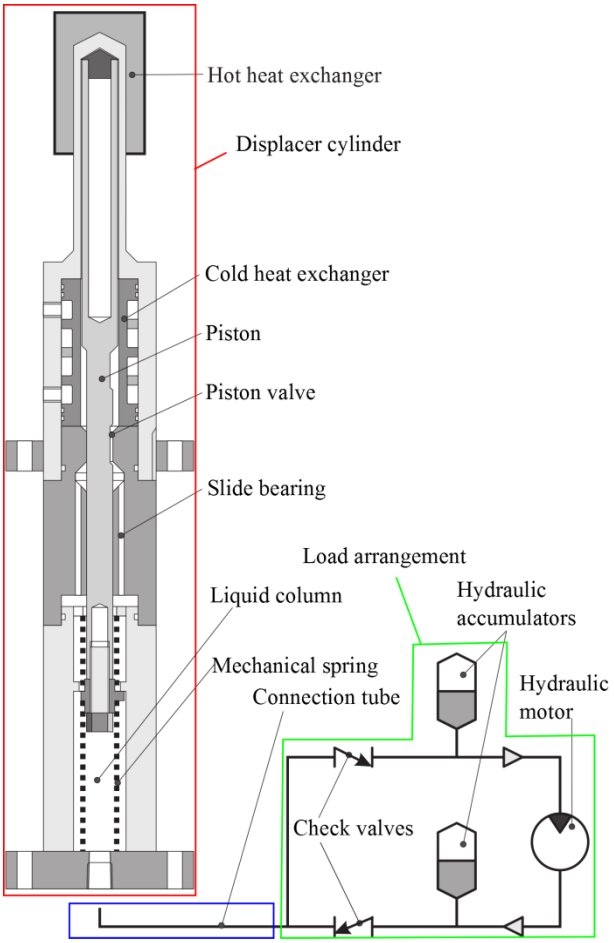


Figure 1 Schematic of Up-THERM engine with piston at TDC

Assuming a cycle to start at the top dead centre (TDC) of the piston (with the piston valve open), the liquid-vapour interface (or liquid level) is in contact with the hot heat exchanger (HHX) surface and the mechanical spring is maximally compressed. Liquid working fluid evaporates, thus increasing the pressure in the gas-spring space. This, along with the mechanical spring, acts to drive a downward displacement of the liquid level and solid piston within the displacer cylinder. Fluid flows from the chamber above the piston valve into the chamber below and the adjacent connection tube. As the piston moves further downwards, the piston valve closes and prevents fluid from exiting the upper chamber. A pressure difference between upper and lower chambers is created as the upper-chamber pressure increases. As the piston continues its downward movement, the valve re-opens and the pressures below and above the valve are suddenly equalized as fluid flows through the valve.

Due to the inertia of the piston and fluid, the liquid level and piston overshoot their equilibrium position halfway between both heat exchangers. While this is taking place, the cold heat exchanger (CHX) becomes exposed to hot vapour which begins to condense and the mechanical spring is compressed. The decreasing pressure and mechanical spring exert restoring forces onto the piston and liquid level, which eventually lead to a reversal of the downwards motion at the bottom dead centre (BDC). The valve closes again, creating a similar pressure difference between the upper and lower chambers as before, after which it re-opens. At this point, fluid flows upwards through the valve and the pressure is equalized. The liquid level and piston overshoot their equilibrium position due to their inertia. The liquid level reaches the HHX again, evaporation increases the pressure and the mechanical spring is compressed. This gradually slows down the piston and liquid levels until their displacement is reversed at the TDC and one full cycle is complete.

During the cycle fluid flows back and forth from the connection tube into and out of the load arrangement. The two check valves transform the oscillatory into a unidirectional flow, while the two hydraulic accumulators act to dampen the flow and pressure oscillations in the load circuit. Finally, the flow is supplied to the hydraulic motor for conversion to electricity.

MODEL DEVELOPMENT

Our modelling methodology follows earlier approaches used by Huang and Chuang [11], Backhaus and Swift [3,12] and Markides and Solanki [5-8] for thermoacoustic and thermofluidic devices. Electrical analogies are drawn such that each linear component can be represented by a resistor, capacitor, inductor or a suitable combination of these. In particular, the series of models developed in Refs. [5-8] for the NIFTE, which is the closest device to the Up-THERM engine given the existence of phase-change heat exchange between a pair of hot/cold heat exchangers and the working fluid, showed close agreement with experimental data. Therefore, this approach is assumed to be a suitable starting point for the Up-THERM concept.

For each component, a set of first-order spatially lumped sub-models are developed, which describe the dominant thermal or fluid process in that component with an ordinary differential equation (ODE). For the piston, slide bearing, liquid column, connection tube, hydraulic accumulators and hydraulic motor

these sub-models are linearized assuming small variations around an operating equilibrium point (in fact, small errors due to the this assumption). The behaviour of the piston valve and check valves is inherently non-linear. Furthermore, the temperature profile in the heat exchangers is assumed to be non-linear. For the gas spring two sub-models are derived: one linearized (LG) and one non-linear (NLG). The sub-models of every component are interconnected to an electrical circuit diagram (shown in Figure 3) in the same way as in the physical engine.

Linear components

The liquid flows in the connection tube and the displacer cylinder are modelled by using a force balance on the liquid volumes. Quasi-steady, laminar and fully developed flow is assumed as the Reynolds and Wormersley numbers are sufficiently low. Viscous drag is represented by resistances, fluid inertia by inductances and hydrostatic pressure difference by capacitances (in the displacer cylinder only):

$$R = \frac{128\mu l_0}{\pi d^4}\ ;\ L = \frac{\rho l_0}{A}\ ;\ C = \frac{A}{\rho g}\,, \tag{1}$$

where μ and ρ are the dynamic viscosity and density of the liquid working fluid; l_0 the length, d the diameter and A the cross-sectional area of the liquid column in equilibrium; and g is the gravitational acceleration.

The piston and leakage flow around it are modelled linearly with the exception of the piston valve (see next section). To derive the electrical analogies, the Navier-Stokes equation for the leakage flow and the force balance for the piston are combined. In the slide bearing the piston and the fluid flow are separated. The fluid flows through two channels and is modelled as a liquid column. Due to the constant height of the slide bearing the hydrostatic pressure difference is neglected. The piston is surrounded by a thin lubricating working fluid film and experiences drag in the slide bearing. The electrical analogies for the piston, leakage flow and slide bearing are as follows:

$$\begin{gathered}
R_{\mathrm{l},1} = \frac{128c_2h_\mathrm{p}\mu}{\pi c_1 c_3}\ ;\ R_{\mathrm{l},2} = \frac{128c_2h_\mathrm{p}\mu}{\pi c_1\left(c_1 - 2c_2d_\mathrm{p}^2\right)}\ ; \\
C_\mathrm{l} = \frac{\pi^2 c_1\left(c_1 - c_2d_\mathrm{p}^2\right)}{64c_2^2k_\mathrm{ms}}\ ;\ L_\mathrm{l} = \frac{64c_2^2m_\mathrm{p}}{\pi^2 c_1\left(c_1 - 2c_2d_\mathrm{p}^2\right)}\ ; \\
R_\mathrm{p} = \frac{64h_\mathrm{p}\mu}{\pi d_\mathrm{p}^2 c_1}\ ; C_\mathrm{p} = \frac{\pi^2 d_\mathrm{p}^2 c_1}{32k_\mathrm{ms}c_2}\ ; L_\mathrm{p} = \frac{32c_2m_\mathrm{p}}{\pi^2 d_\mathrm{p}^2 c_1}\ ; \\
R_{\mathrm{b,p}} = \frac{16l_\mathrm{b}\mu}{\pi^2\delta d_\mathrm{p}^3}\ ; L_{\mathrm{b,p}} = \frac{4\rho_\mathrm{ss}l_\mathrm{b}}{\pi d_\mathrm{p}^2}\ ; R_{\mathrm{b,l}} = \frac{128\mu l_\mathrm{b}}{\pi d_{\mathrm{b,l}}^4}\ ; \\
L_{\mathrm{b,l}} = \frac{\rho l_\mathrm{b}}{A_{\mathrm{b,l}}}\,.
\end{gathered} \tag{2}$$

In Eq. (2) h_p, m_p and d_p are the height, mass and diameter of the piston, l_b, d_b, and A_b the length of the slide bearing, the diameter and cross-sectional area of the channels, k_ms and ρ_ss the spring constant of the mechanical spring and the density of the piston. Furthermore, three geometric constants are used: $c_1 = d_\mathrm{c}^2 - d_\mathrm{p}^2$, $c_2 = \ln\left(d_\mathrm{c}/d_\mathrm{p}\right)$ and $c_3 = c_2\left(d_\mathrm{c}^2 + d_\mathrm{p}^2\right) - c_1$, with d_c the diameter of the cylinder.

The linear model (LG) of the gas spring in the displacer cylinder and the hydraulic accumulators are modelled by linearizing the ideal-gas law that results a capacitance:

$$C = \frac{V_0}{\gamma P_0}\,, \tag{3}$$

where P_0 is the pressure and V_0 the volume of the gas spring at equilibrium, and γ the ratio of heat capacities.

The losses and inductance in the hydraulic motor are modelled by using a torque balance on the motor. This results in a resistance and an inductance:

$$R_\mathrm{hm} = \frac{16\mu_\mathrm{lub}d_\mathrm{s}^3 l_\mathrm{s}}{\pi\epsilon d^4 d_\mathrm{m}^2}\ ;\ L_\mathrm{hm} = \frac{8m_\mathrm{m}}{\pi^2 d^4}\,. \tag{4}$$

In the above equation μ_lub is the dynamic viscosity of the lubricant around the shaft, d_s and l_s the shaft diameter and length, ϵ the gap between the shaft and motor, d and d_m the diameter of the inlet pipe and motor and m_m the uniformly distributed rotating mass of the motor. The power P_el that can be extracted from the cycle, when the flow rate U_hm flows through the hydraulic motor, is dissipated in the resistance R_gen. Using Ohm's law the power can be calculated from:

$$P_\mathrm{el} = R_\mathrm{gen}U_\mathrm{hm}^2\,, \tag{5}$$

where R_gen is determined empirically.

Non-linear components

The non-linear model of the gas spring uses the ideal-gas law:

$$C = \frac{\gamma(P_0 + P_\mathrm{v})}{V_0 + V_\mathrm{v}}\,, \tag{6}$$

with the constant equilibrium pressure P_0 and volume V_0 and the time varying pressure P_v and volume V_v.

The temperature profile in the heat exchangers is modelled by assuming that the temperature on the heat exchanger walls will saturate when the vapour liquid interface moves far away from the equilibrium (mid-stroke) position [13]. Such a temperature profile can be described by the static relationship:

$$T_\mathrm{hx} = \alpha\tanh(\beta y)\,, \tag{7}$$

where α is half the maximum temperature difference between the hot and cold heat exchangers, $\alpha\beta$ the gradient in the origin and y the height of the vapour liquid interface. A graphical illustration of the temperature profile can be seen in Figure 2.

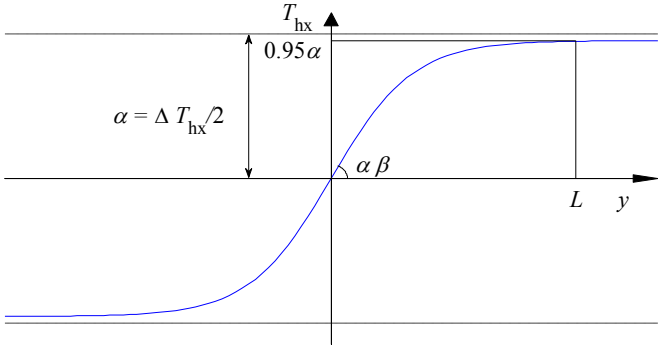


Figure 2 Imposed temperature profile on heat exchanger walls, with values for constants taken from experimental data

The piston valve is modelled by a Heaviside step function H{.}:

$$R_{\mathrm{pv}} = R_{\mathrm{min}} + R_{\mathrm{max}}\left(-\mathrm{H}\{P_{\mathrm{C,d}} - \rho g h_{\mathrm{v}}\} + \mathrm{H}\{P_{\mathrm{C,l,dc}} + \rho g h_{\mathrm{v}}\}\right) \quad (8)$$

where $P_{\mathrm{C,d}}$ is the hydrostatic pressure in the displacer cylinder liquid column, ρ the working fluid density, g the gravitational acceleration and h_{v} the piston position where the valve opens and closes, respectively, R_{min} the constant fluid-flow resistance of the valve (see Eq. (1)) and R_{max} a large pre-set constant.

The two check valves in the load arrangement are also modelled using Heaviside functions. Depending on the direction of the flow through a check valve, it is either open or closed:

$$R_{\mathrm{cv}} = R_{\mathrm{max,cv}}\mathrm{H}\{U\}\,, \quad (9)$$

where $R_{\mathrm{max,cv}}$ is a constant and very high resistance, and U the flow rate through the check valve.

Furthermore, the non-linear resistance R_{nl} is introduced in the displacer cylinder. It is necessary to guarantee that the amplitudes of the displacements of the solid piston and the liquid column in the displacer cylinder are not larger than the length of the displacer cylinder. It has the form:

$$R_{\mathrm{nl}} = R_{\mathrm{max,3}}\left(H\{P_{\mathrm{C,d}} - \rho g h_3\} + H\{-P_{\mathrm{C,d}} - \rho g h_3\}\right). \quad (10)$$

In the above equation h_3 is the maximum amplitude of the liquid column. By reaching that height, the value for R_{nl} becomes large and thus blocks the piston and fluid flow. The effect in the physical engine is that the piston/liquid column impacts a wall and cannot move further.

By connecting all sub-models in the same way as they are in the physical engine (Figure 1), one obtains the electrical circuit diagram shown in Figure 3. A description and the nominal values of the resistances, inductances and capacitances in the circuit shown in Figure 3 can be found in Table 1.

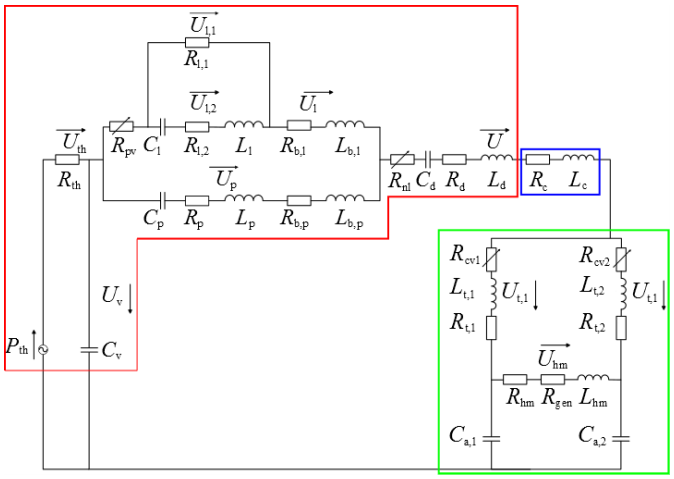


Figure 3 Electrical circuit diagram of the Up-THERM engine; colours correspond to the engine parts in Figure 1

Due to the (relatively) small temperature difference between heat source and heat sink, the thermal efficiency of the engine is lower than that expected for high-grade heat converters. The efficiency of the engine is thereby compared with that of an ideal Carnot cycle using the exergy (second law) efficiency, i.e. the ratio of the thermal efficiency to the Carnot efficiency. It is calculated with the following equation:

$$\eta_{\mathrm{ex}} = \frac{\int R_{\mathrm{gen}} U_{\mathrm{hm}} \mathrm{d}V_{\mathrm{hm}}}{\int P_{\mathrm{th}} \mathrm{d}V_{\mathrm{th}}}. \quad (11)$$

In the above equation $V_{\mathrm{hm}} = \int U_{\mathrm{hm}} \mathrm{d}t$ is the volumetric displacement in the hydraulic motor in one cycle and $V_{\mathrm{th}} = \int U_{\mathrm{th}} \mathrm{d}t$ the (equivalent) entropy flow due to thermal energy transfer to the working fluid during one cycle.

Table 1 Nominal values of RLC components shown in Figure 3

Resistances [kg/m⁴s]	Thermal resistance	R_{th}	6.58×10^{7}
	Piston	R_{p}	9.86×10^{4}
	Leakage flow 1	$R_{\mathrm{l,1}}$	6.23×10^{7}
	Leakage flow 2	$R_{\mathrm{l,2}}$	1.28×10^{6}
	Piston in slide bearing	$R_{\mathrm{b,p}}$	7.74×10^{5}
	Fluid flow in slide bearing	$R_{\mathrm{b,l}}$	5.31×10^{7}
	Displacer cylinder flow	R_{d}	2.20×10^{7}
	Connection tube flow	R_{c}	1.07×10^{3}
	Flow in load pipes	$R_{\mathrm{t,1}}$, $R_{\mathrm{t,2}}$	2.86×10^{6}
	Hydraulic motor friction	R_{hm}	3.33×10^{8}
	Power generation	R_{gen}	3.32×10^{8}
Inductances [kg/m⁴]	Piston	L_{p}	5.96×10^{6}
	Leakage flow	L_{l}	6.45×10^{7}
	Piston in slide bearing	$L_{\mathrm{b,p}}$	3.01×10^{6}
	Fluid flow in slide bearing	$L_{\mathrm{b,l}}$	9.18×10^{6}
	Displacer cylinder flow	L_{d}	9.50×10^{7}
	Connection tube flow	L_{c}	2.97×10^{5}
	Flow in load pipes	$L_{\mathrm{t,1}}$, $L_{\mathrm{t,2}}$	2.80×10^{6}
	Hydraulic motor	L_{hm}	2.37×10^{6}
Capacitances [m⁴s²/kg]	Gas spring	C_{v}	4.05×10^{-11}
	Piston	C_{p}	6.02×10^{-10}
	Leakage flow	C_{l}	1.78×10^{-10}
	Displacer cylinder	C_{d}	8.05×10^{-9}
	Hydraulic accumulators	$C_{\mathrm{a,1}}$, $C_{\mathrm{a,2}}$	1.79×10^{-9}

RESULTS AND DISCUSSION

We evaluate three performance indicators of the Up-THERM engine: frequency, power output and exergy efficiency. The three indicators are calculated at equilibrium/back-pressures between 5 bar and 25 bar. The selected working fluid is water, although organic working fluids such as alkanes or refrigerants can be used. Figure 4-6 show the results for the Up-THERM engine model with both the linear and the non-linear gas spring models.

Figure 4 shows the oscillation (i.e. operation) frequency of the engine. It can be seen that the frequency of the LG model is higher than that of the NLG model. For the former model, the frequency rises from 4.1 Hz at 5 bar to 5.0 Hz at 25 bar. The frequency of the latter model stays almost constant at 0.1 Hz. Given experimental results from a prototype engine similar to the Up-THERM that showed a frequency between 0.02 and 0.2 Hz for back-pressures between 5 bar and 22 bar [14], as well as experimental values obtained for the NIFTE [7], it is concluded that the non-linear gas spring model is capable of predicting realistic frequencies for an operating Up-THERM device.

Furthermore, the power output for different back-pressures is shown in Figure 5 for the two models. The NLG model has a constant power output of approximately 3 W over the investigated back-pressure range. The power output of the LG model increases from 1.4 W (at 5 bar) to 264 W (at 25 bar).

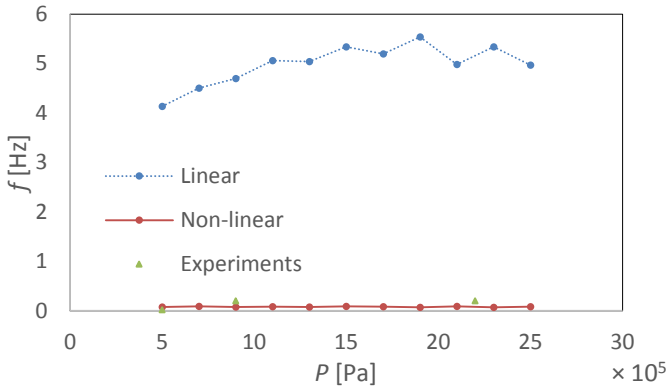


Figure 4 Oscillation frequency for different back-pressures; linear, non-linear gas spring models and experimental values from Ref. [14]

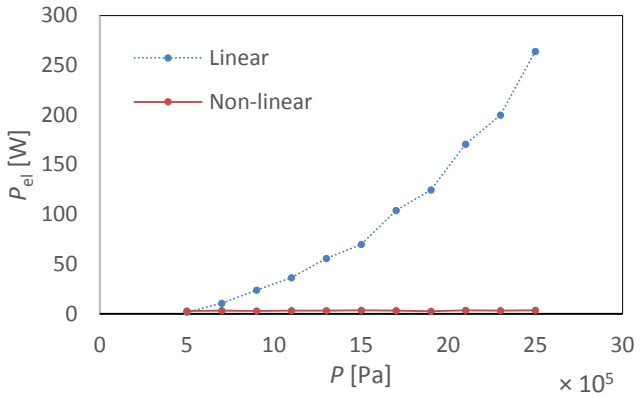


Figure 5 Power output for different pressures of the model with the linear and non-linear gas spring

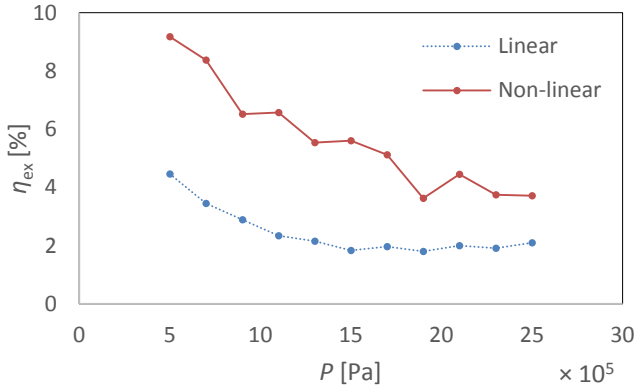


Figure 6 Exergy efficiency for different pressures of the model with the linear and non-linear gas spring

The exergy efficiency for different back-pressures is shown in Figure 6, with the non-linear model predicting higher exergy efficiencies even though the power output of the linear model was higher (see Figure 5), suggesting that this higher power out is also associated with a significantly increased thermal (and exergy) input into the device at progressively higher back-pressures. Specifically, for the NLG model, the exergy efficiency decreases from 9.1% at 5 bar to 3.7% at 25 bar, whereas for the LG model the efficiency lies between 2% and 4.5% over the entire investigated back-pressure range.

Based on experimental experience, the NLG seems to predict more realistic operation frequencies (Figure 4) and, therefore, a parametric study will be performed by using this model. We investigate the influence of six geometric properties on the three performance indicators: the length and diameters of the liquid columns in the displacer cylinder (l_d and d_d) and connection tube (l_c and d_c), the diameter of the tube in the load arrangement d_t, and the height of the gas spring h_v. The six physical dimensions are successively varied between 10% and a factor of 10 times of their nominal values (based on the current prototype design) while the other dimensions are kept at their nominal values. The results are shown in Figures 7-9; the superscript '*' indicates values normalized by their respective nominal values. It should be noted that for the displacer cylinder diameter d_d a limit cycle (i.e. sustained, persistent operation) could only be achieved for values between 10% and 100% of its nominal value.

In Figure 7 the frequency of oscillation is plotted against all varying physical dimensions. It can be seen that increasing the value of almost all of the physical dimensions does not have a significant effect on the frequency. The frequency increases slightly when the gas spring height h_v is reduced below 25% of its nominal value. By reducing the displacer cylinder diameter d_d below 40% of its nominal value, the increase in frequency is steeper. At these higher frequencies it may be expected that, with everything else the same, the pumped volumetric flow-rates in the hydraulic load will be higher leading to higher power outputs. The results in Figure 8, however, reveal that this is not the case.

Specifically, Figure 8 shows the corresponding variations of the power output plotted for different values of the same physical dimensions as in Figure 7. The power output increases when the displacer cylinder length l_d is increased, which allows for larger amplitudes of oscillations of the liquid column and hence larger flow rates through the hydraulic motor. Decreasing the height of the gas spring h_v also increases the power output, while decreasing the diameter of the displacer cylinder d_d and of the tube in the load arrangement d_t decreases the power output. The dimensions of the connection tube do not have an effect on the power output of the engine. It is therefore concluded, in conjunction with Figure 7, that an increased volumetric displacement (e.g. by scaling-up the device) may (in the case of the displacer cylinder) or may not (in the case of the height of the gas spring) lead to increased power outputs, which in fact result from the product of this volumetric displacement and the frequency of oscillation in Figure 7.

Figure 9 shows the exergy efficiency values corresponding to Figures 7 and 8. At low values of the diameter of the displacer cylinder d_d the efficiency drops sharply. Decreasing the diameter of the tube in the load arrangement d_t below 40% of its nominal value, also leads to a decrease in efficiency. The efficiency increases if the length of the displacer cylinder and the height of the gas spring are increased. The remaining physical dimensions do not have significant influence on the exergy efficiency of the engine.

Together, Figure 7-9 indicate that the dimensions of the connection tube have little influence on the performance indicators of the engine. The performance is most influenced by the height of the gas spring h_v, the displacer cylinder diameter d_d and length l_d. Also, it is important to note that high power outputs and efficiencies do not arise from the same engine designs, suggesting that a compromise is necessary depending on the application.

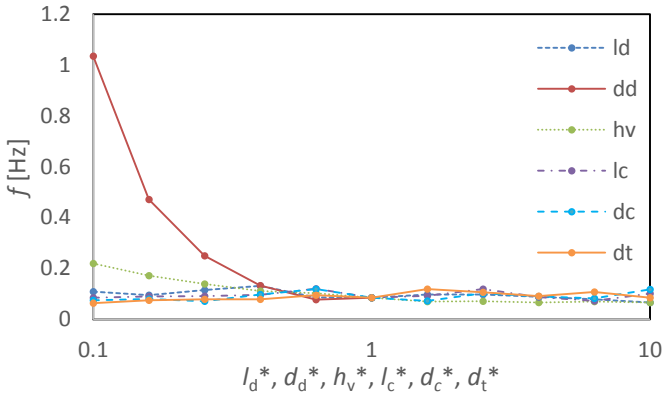


Figure 7 Influence of physical dimensions on frequency

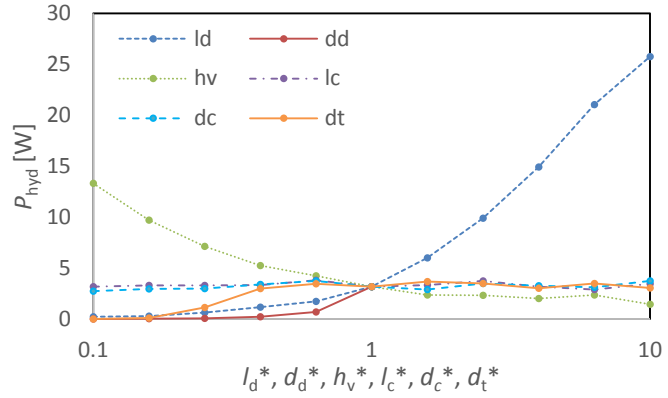


Figure 8 Influence of physical dimensions on power output

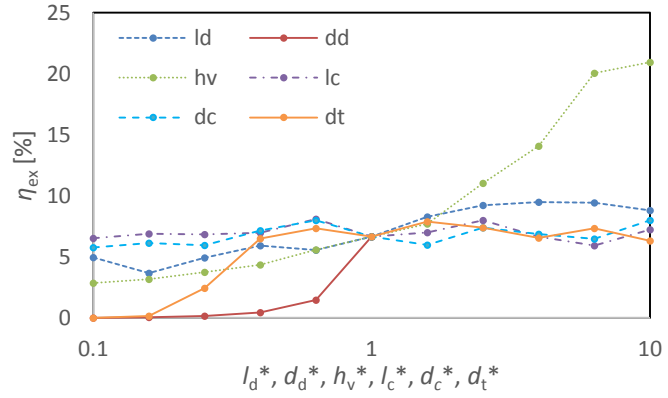


Figure 9 Influence of physical dimensions on exergy efficiency

CONCLUSION

A theoretical model of a new two-phase thermofluidic oscillator termed Up-THERM has been developed. The engine consists of a displacer cylinder with a solid piston and a pair of hot and cold heat exchangers. Furthermore, it comprises a hydraulic-circuit load arrangement with a hydraulic motor. Periodic phase-change leads to the vertical reciprocating displacement of the solid piston, as well as sustained, persistent oscillations in the pressure, volume and flow-rate of the working fluid which are harnessed in the load arrangement to produce work.

The Up-THERM engine model consists of a set of first-order, spatially lumped ordinary differential equations that are linearized for some components. However, components which have a crucial impact on the operation and performance of the engine are described non-linearly. Two versions of the model were compared: one including a linear description of the working-fluid (vapour space) gas spring (LG) and one with a non-linear description (NLG). The non-linear description delivered more realistic predictions of the frequency compared to experimental values from prototypes under current testing.

For a 'nominal' Up-THERM device, exergy efficiency values up to about 10% were demonstrated. A parametric study was also performed using the non-linear gas spring model. It was shown that for an increased power output the displacer cylinder should be lengthened and/or the height of the gas spring reduced. The efficiency can be increased further by increasing the length of the displacer cylinder and/or the height of the gas spring.

ACKNOWLEDGMENT

The research leading to these results has received funding from the 7th Framework Programme of the European Commission, grant agreement number 605826.

REFERENCES

[1] Stammers C.W., The operation of the Fluidyne heat engine at low differential temperatures, *Journal of Sound and Vibration*, Vol. 63, No. 4, 1979, pp. 507-516

[2] West C.D., and Pandey R.B., Laboratory prototype Fluidyne water pump, *Proceedings of the 16th Intersociety Energy Conversion Engineering Conference (IECEC 81)*, Atlanta, USA, August 1981

[3] Backhaus S., and Swift G.W., A thermoacoustic-Stirling heat engine: detailed study, *Journal of the Acoustical Society of America*, Vol. 107, No. 6, 2000, pp. 3148-3166

[4] Ceperley P.H., A pistonless Stirling engine - the travelling wave heat engine, *Journal of the Acoustical Society of America*, Vol. 66, No. 5, 1979, pp. 1508-1513

[5] Markides C.N., and Smith T.C.B., A dynamic model for the efficiency optimization of an oscillatory low grade heat engine, *Energy,* Vol. 36, No. 12, 2011, pp. 6967-6980

[6] Solanki R., Galindo A., and Markides C.N., Dynamic modelling of a two-phase thermofluidic oscillator for efficient low grade heat utilization: Effect of fluid inertia, *Applied Energy*, Vol. 89, No. 1, 2012, pp.156-163

[7] Solanki R., Mathie R., Galindo A., and Markides C.N., Modelling of a two-phase thermofluidic oscillator for low-grade heat utilisation: accounting for irreversible thermal losses, *Applied Energy*, Vol. 106, 2013, pp. 337-354

[8] Solanki R., Galindo A., and Markides C.N., The role of heat exchange on the behaviour of an oscillatory two-phase low-grade heat engine, *Applied Thermal Engineering,* Vol. 53, No. 2, 2013, pp. 507-516

[9] Glushenkov M., Sprenkeler M., Kronberg A., Kirillov V., Single-piston alternative to Stirling engines, *Applied Energy*, Vol. 97, 2012, pp.743-748

[10] Roestenberg T., Glushenkov M.J., Kronberg A.E., Krediet H.J., and vd Meer Th.H., Heat transfer study of the pulsed compression reactor, *Chemical Engineering Science*, Vol. 65, No. 1, 2010, pp. 88-91

[11] Huang B.J., and Chuang M.D., System design of orifice pulse-tube refrigerator using linear flow network analysis, *Cryogenics*, Vol. 36, No. 11, 1996, pp. 889-902

[12] Backhaus S., and Swift G.W., A thermoacoustic Stirling heat engine, *Letters to Nature*, Vol. 399, 1999, pp. 335-338

[13] Markides C.N., Osuolale A., Solanki R., and Stan G.-B.V., Nonlinear heat transfer processes in a two-phase thermofluidic oscillator, *Applied Energy*, Vol.104, 2013, pp. 958-977

[14] Taleb A.I., Kirmse C.J.W., Oyewunmi O.A., Samoilov A., Kirillov V.A., and Markides C.N., An investigation of a new phase-change reciprocating-piston heat engine, *Proceedings of the 3rd Sustainable Thermal Energy Management Network International Conference (SusTEM 2015)*, Newcastle, United Kingdom, July 2015